Quality Assurance of Chapter 11: Requirements on Upper Shelf Energy

This report documents the results of the quality assurance (QA) task for Chapter 11 of the draft technical basis NUREG for the risk-informed Appendix G project. Chapter 11 discusses the derivation of updated minimum upper shelf energy (USE) requirements for reactor vessels. The quality assurance effort for this chapter involved three specific subtasks: (1) confirming the validity of stress intensity factor equations used in Regulatory Guide (RG) 1.161, (2) verifying calculations of minimum USE based upon the RG 1.161 methodology, (2) verifying Fracture Analysis of Vessels-Oak Ridge (FAVOR) runs used to calculate minimum USE.

RG 1.161 Methodology

Proper Calculation Procedures

RG 1.161 provides equations for calculating (1) the applied J-integral, or J, for a reactor vessel subject to certain loading conditions and (2) the vessel material's resistance to ductile tearing, or J_R. To calculate J, one first must determine the mode I stress intensity factors (SIFs) due to pressure and thermal stress. The equations used to do that were derived from finite element modeling results and are shown in Equations 1-6.

$$K_{Ip}^{Axial} = (SF)p_a[1 + R_i/t](\pi a)^{0.5}F_1 \quad \text{Equation 1}$$

$$F_1 = 0.982 + 1.006(a/t)^2 \quad \text{Equation 2}$$

$$K_{Ip}^{Circum} = (SF)p_a[1 + R_i/(2t)](\pi a)^{0.5}F_2 \quad \text{Equation 3}$$

$$F_2 = 0.885 + 0.233(a/t) + 0.345(a/t)^2 \quad \text{Equation 4}$$

$$K_{It} = [(CR)/1000]t^{2.5}F_3 \quad \text{Equation 5}$$

$$F_3 = 0.69 + 3.127(a/t) - 7.435(a/t)^2 + 3.532(a/t)^3 \quad \text{Equation 6}$$

where K_{Ip}^{Axial} is the SIF due to internal pressure for an axial flaw, K_{Ip}^{Circum} is the SIF due to pressure for a circumferential flaw, K_{It} is the SIF due to thermal stress, SF is the safety factor, p_a is the maximum accumulation pressure, a is the crack depth, and t is the vessel thickness. K_{Ip}^{Axial} is always larger than K_{Ip}^{Circum}, so Equation 1 was used for all the calculations in this work. Equations 1 and 3 are valid for $0.05 \leq a/t \leq 0.50$, while Equation 5 is valid for $0.2 \leq a/t \leq 0.5$ and $0 \leq CR \leq 100$°F/hr. The next step to calculate J is to determine the effective flaw depth for small scale yielding, a_e (Equation 7).

$$a_e = a + \frac{1}{6\pi}\left[\frac{K_{Ip} + K_{It}}{\sigma_y}\right]^2 \quad \text{Equation 7}$$

K_{Ip}^{Axial} and K_{It} are then recalculated with a_e substituted for a in Equations 1-6, yielding K_{Ip}' and K_{It}'. K_{Ip}' and K_{It}' are used in Equation 8 to calculate J.

$$J = 1000\left(K_{Ip}' + K_{It}'\right)^2/E' \quad \text{Equation 8}$$

where $E' = E/(1 - \nu^2)$, E is the elastic modulus, and ν is Poisson's ratio.

The equations for J_R are based upon correlations developed via least squares nonlinear curve fitting of experimental data. They take the form of Equation 9.

$$J = C1(\Delta a)^2 exp[C3(\Delta a)^{C4}] \quad \text{Equation 9}$$

The form of the parameter C1 depends upon the choice of model: Charpy Model, Cu-ϕt Model, or CVN_p Model. This work utilized the Charpy model, which follows Equations 10-12.

$$\ln C1 = a_1 + a_2 \ln CVN + a_3 T + a_4 \ln B_n \quad \text{Equation 10}$$

$$C2 = d_1 + d_2 \ln C1 + d_3 \ln B_n \quad \text{Equation 11}$$

$$C3 = d_4 + d_5 \ln C1 + d_6 \ln B_n \quad \text{Equation 12}$$

where a_i and d_i are fitting parameters tabulated in **ref**, CVN is Charpy V-notch impact energy, T is temperature, and B_n is specimen thickness.

The RG 1.161 methodology involves applying two criteria to determine a minimum USE, based upon the calculation of J and J_R. The first criterion mathematically states that the postulated crack (a = 0.25t, in this case) must not initiate at 0.1 in. ductile crack extension (Equation 13).

$$J \leq J_R \text{ when } \Delta a = 0.1 \text{ in.} \quad \text{Equation 13}$$

This criterion is evaluated with SF = 1.15. The second criterion states that a 0.25t flaw must exhibit stable ductile tearing (i.e., it may initiate but it must subsequently arrest) when SF = 1.25, as in Equation 14.

$$\frac{\partial J}{\partial a} \leq \frac{\partial J_R}{\partial a} \text{ when } J = J_R \quad \text{Equation 14}$$

Practically, one must solve Equation 15 to demonstrate compliance with Equation 13.

$$J - J_R = 0 \text{ or } J = J_R \quad \text{Equation 15}$$

J_R, according to Equations 9-12, is a function of CVN. The difference $J-J_R$ is, therefore, also a function of CVN and solving Equation 15 is equivalent to finding the zero of that function. The solution is the lowest USE value that satisfies Equation 13. Various numerical methods exist to find the zero of a nonlinear function. The method employed in this work was Matlab's built-in "fsolve" command, which can apply one of several different algorithms to solve the problem.

Demonstrating compliance with Equation 14 is less straight forward. The problem may be restated as follows. "Find the CVN value that leads to the J and J_R curves tangent to one another." When two functions are tangent to each other, two conditions hold true simultaneously: the functions are equal and their derivatives are equal. For this particular application, the mathematical statement of the problem is found in Equations 16 and 17, respectively.

$$J - J_R = 0 \quad \text{Equation 16}$$

$$\frac{\partial J}{\partial a} - \frac{\partial J_R}{\partial a} = 0 \qquad \text{Equation 17}$$

The proper solution to the problem, therefore, involves successive analytical differentiation of Equations 1-12. While this task is non-trivial, it is possible with due care. In particular, defining constants that do not depend upon Δa (or, equivalently a) or CVN simplifies the process. The differentiation is found in the Appendix. Equations 16 and 17, once they have been properly derived, form a system of two simultaneous nonlinear equations with two unknowns: CVN and Δa. The solution is the lowest USE value that satisfies Equation 14 and the Δa where J and J_R are exactly tangent. Matlab's "fsolve" command can also numerically solve this system of equations.

The above discussion outlines the steps necessary to determine USE values that satisfy Equations 13 and 14, USE_1 and USE_2, respectively. The correct minimum USE is then the greater of the two.

Confirmation of SIF Equations

The technical basis behind Equations 1 and 5 are found in references x and y. However, these documents show that they were developed for $R_i/t = 10$, which is typical of pressurized water reactors but not boiling water reactors (where R_i/t is typically 20). This section of the report describes an effort to verify the validity of Equation 1 and 5 when $R_i/t = 20$.

Two methods were employed to independently calculate SIF and compare it to Equations 1 and 5: American Petroleum Institute (API) standard 579 and the method employed in FAVOR. Both methods utilize tabulated influence coefficients, which are determined from finite element analysis. For the API-579 method, the entire through-wall stress distribution is fit by a 4th order polynomial (Equation 18)

$$\sigma(x) = \sigma_0 + \sigma_1\left(\frac{x}{t}\right) + \sigma_2\left(\frac{x}{t}\right)^2 + \sigma_3\left(\frac{x}{t}\right)^3 + \sigma_4\left(\frac{x}{t}\right)^4 \qquad \text{Equation 18}$$

where σ_i are fitting coefficients and x is the through-wall distance. The mode I SIF, K_I, is then determined by Equation 19.

$$K_I = \left[\sigma_0 G_0 + \sigma_1 G_1\left(\frac{a}{t}\right) + \sigma_2 G_2\left(\frac{a}{t}\right)^2 + \sigma_3 G_3\left(\frac{a}{t}\right)^3 + \sigma_4 G_4\left(\frac{a}{t}\right)^4\right]\sqrt{\frac{\pi a}{Q}} \qquad \textit{Equation 19}$$

where G_i are the influence coefficients and Q is the flaw-shape parameter given by Equation 20

$$Q = 1 + 1.464\left(\frac{a}{c}\right)^{1.65} \quad for\ a \le c \qquad \text{Equation 20}$$

where c is half the crack length. FAVOR employs a similar approach, except that the stress profile is fit only up to the crack tip as opposed to the entire profile (Equation 21)

$$\sigma(x) = C_0 + C_1(x/a) + C_2(x/a)^2 + C_3(x/a)^3 \qquad \text{Equation 21}$$

SIF is then calculated according to Equation 22.

$$K_I(a) = \sum_{j=0}^{3} C_j K_j^*(a)\sqrt{\pi a} \qquad \text{Equation 22}$$

The through-wall hoop stress distribution, $\sigma_{\theta\theta}(r)$, for a thick-walled cylinder subject to internal pressure is given by Equation 23.

$$\sigma_{\theta\theta}(r) = \frac{pR_i^2}{R_o^2 - R_i^2}\left[1 + \left(\frac{R_o^2}{r}\right)^2\right] \qquad \text{Equation 23}$$

where $R_o = R_i + t$ is the outer radius and r is the radial position from the center. Equation 1 was verified by calculating the through wall stress by Equation 23 and the resulting SIFs by Equations 18-22 for a vessel with R_i = 91.5 in. and t = 4.47 in. (Figure 1).

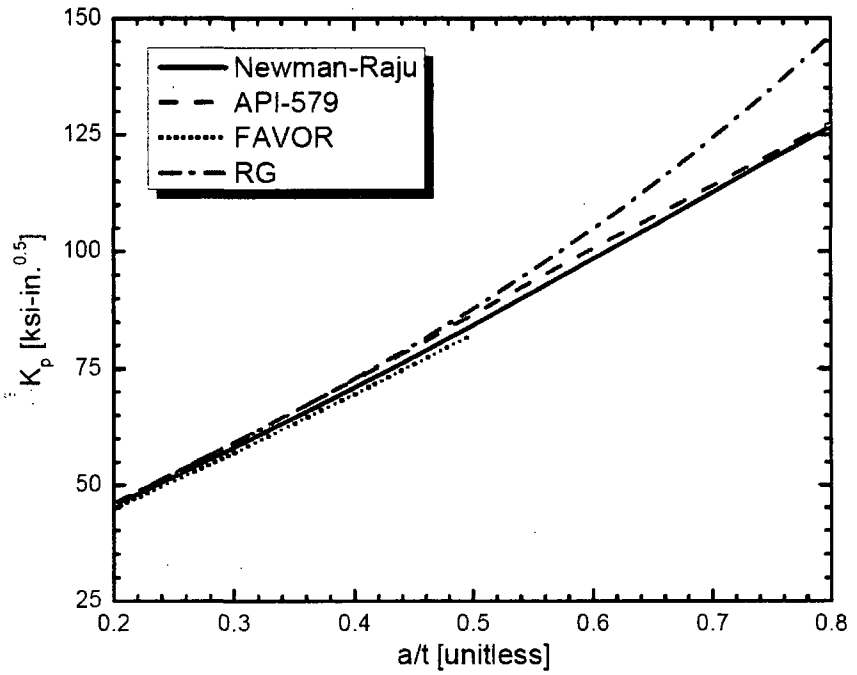

Figure 1: Comparison of the RG 1.161 equation for K_p with three methods.

The Newman-Raju method shown in Figure 1 is the original work upon which Equation 1 is based. Details for that method can be found in reference z. Figure 1 shows that there is reasonable agreement of the RG 1.161 equation for K_I due to pressure with the other methods, even with the boiling water reactor vessel geometry (note: Equation 1 ceases to be valid past a/t = 0.5).

Verifying Equation 5 requires calculating a through-wall temperature distribution and, from there, determining the thermal hoop stress. The technical basis for Equation 5 utilized finite element modeling to solve Equation 24 for T as a function of r and time, τ, during a cooldown transient.

$$\rho c_p \frac{\partial T}{\partial \tau} = \frac{1}{r}\frac{\partial}{\partial r}\left(kr\frac{\partial T}{\partial r}\right) \qquad \text{Equation 24}$$

The boundary conditions for this problem were specified in ref x as Equation 25.

$$q = h_c(T_f - T_s) \qquad \text{Equation 25}$$

where h_c, the heat transfer coefficient, is 1000 BTU/(hr-ft^2-°F) at r = R_i and 0 at r = R_o, T_f is the coolant temperature, and T_s is the temperature at r = R_i. The initial conditions were not specified in the reference x but were taken to be Equation 26.

$$T(r,0) = 550^oF \; for \; all \; r \qquad \text{Equation 26}$$

The remaining inputs for the calculation are contained in Table 1.

Table 1: Material property inputs for determining T(r,τ).

Property	Value
E	2.9 x 10^4 ksi
ν	0.3
α	7.2 x 10^{-6} °F^{-1}
k	22 BTU/(hr-ft-°F)
r	485 lbm/ft^3
c_p	0.128 BTU/(lb$_m$-°F)
CR	100°F/hr

While reference x utilized finite element analysis to solve Equation 24, other methods exist to solve the problem. This work employed Matlab's built-in "pdepe" command to solve Equation 24 for a cooling rate of 100°F/hr to an inner wall temperature of 70°F. Calculated temperature profiles at different times early in the transient are shown in Figure 2.

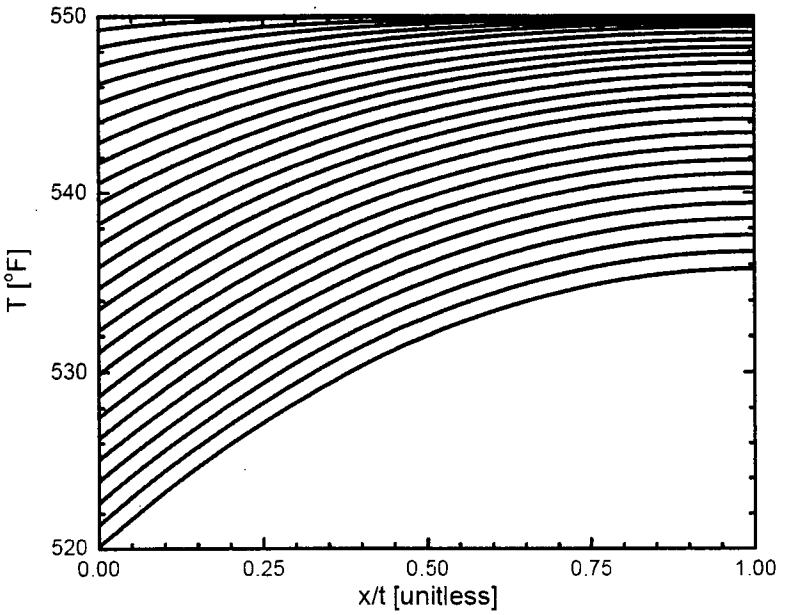

Figure 2: Calculated temperature profiles for the first 20 min of the cooldown transient, shown in 47 s increments.

The thermal hoop stress is given in reference x as Equation 27.

$$\sigma_{\theta\theta}(r,\tau) = \frac{\alpha E}{1-\upsilon}\frac{1}{r^2}\left(\frac{r^2+R_i^2}{R_o^2-R_i^2}\int_{R_i}^{R_o} T(r,t)r\,dr + \int_{R_i}^{r} T(r,\tau)r\,dr - T(r,\tau)r^2\right) \qquad \text{Equation 27}$$

where α is the coefficient of thermal expansion, E is the elastic modulus, and ν is Poisson's ratio. Thermal stress profiles corresponding to the last 4 hours of the cooldown, along with the associated 4th-order polynomial fits, are shown in Figure 3.

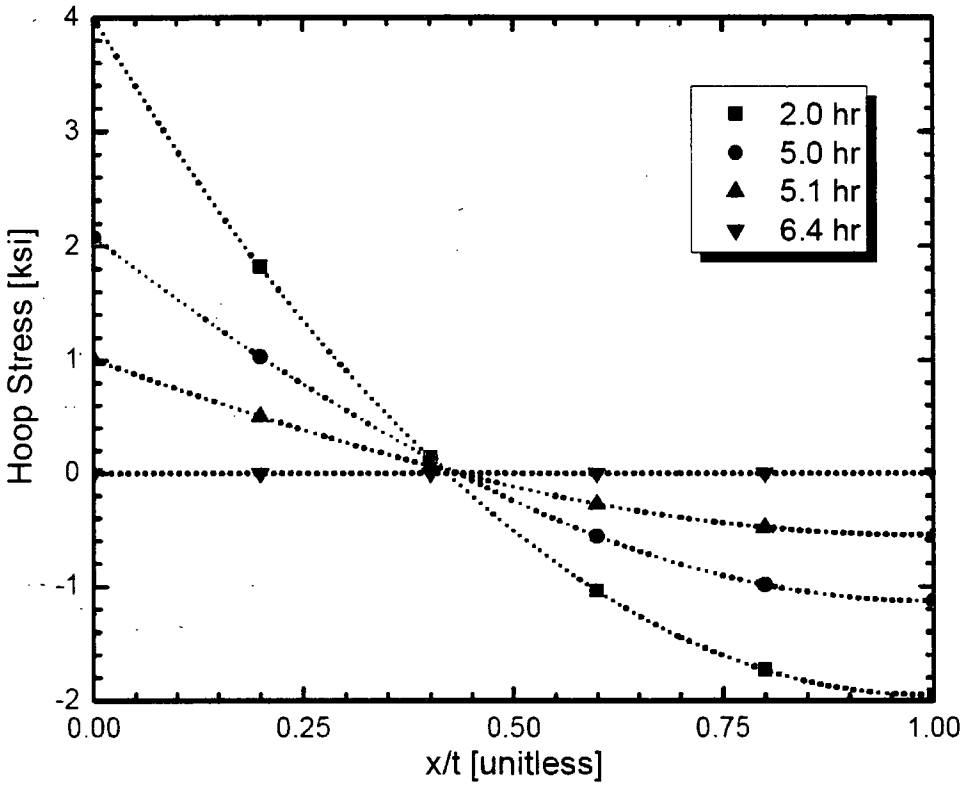

Figure 3: Thermal hoop stress from τ = 2.0 hr to τ = 6.4 hr during the cooldown transient.

K_I according to the API-579 method for a/t = 0.25 is shown as a function of time in Figure 4.

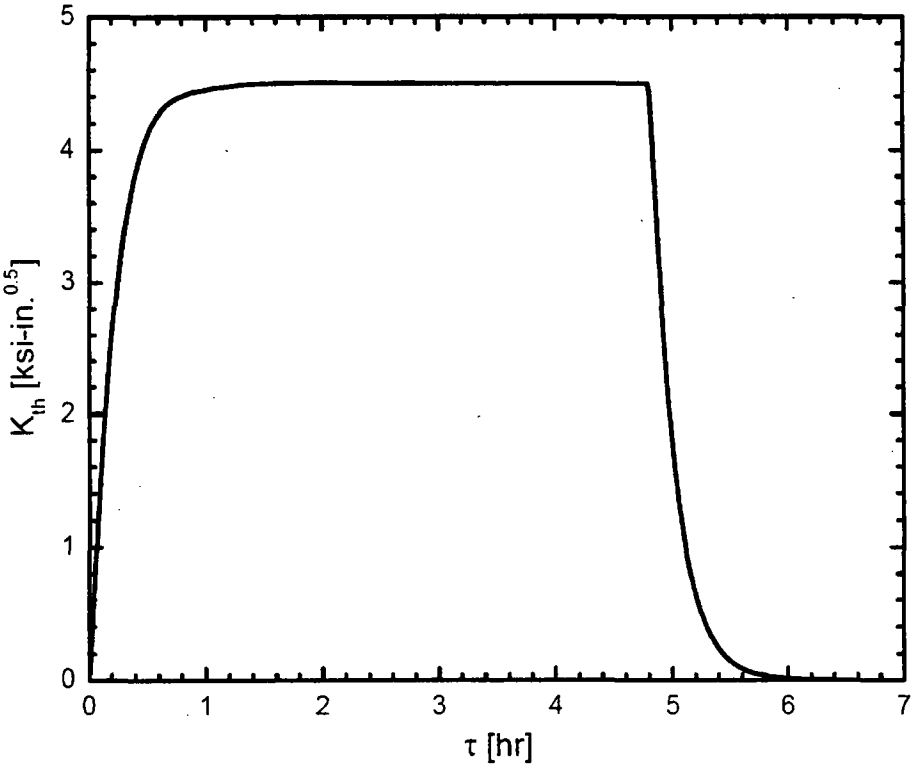

Figure 4: Thermal SIF as a function of time during the cooldown transient.

Finally, the RG 1.161 equation is compared to the K_I determined at τ = 1.7 hrs in Figure 5.

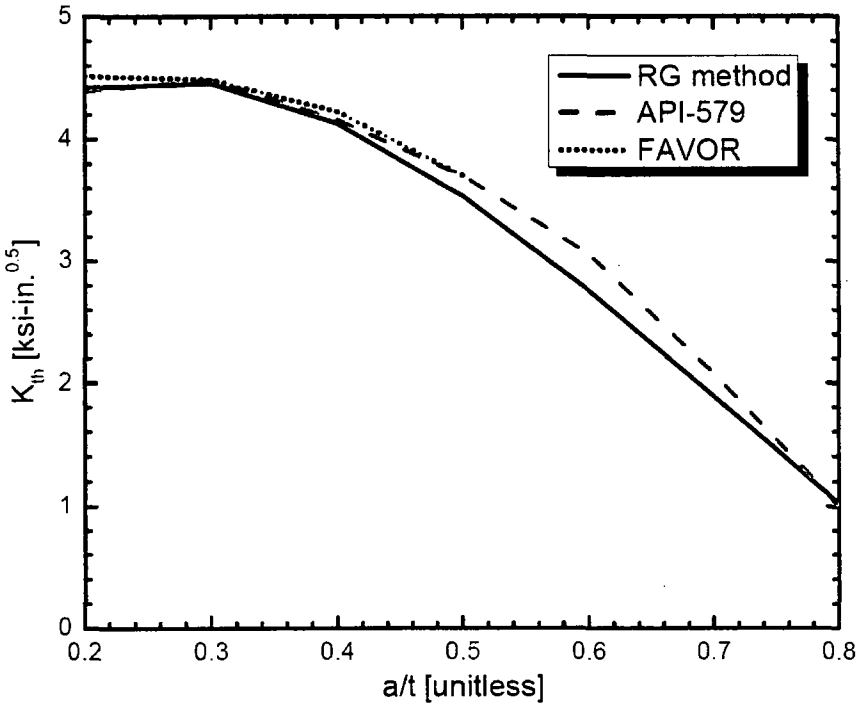

Figure 5: Comparison of the RG 1.161 thermal SIF calculation with two other methods.

Figure 5 shows that the RG 1.161 equation agrees reasonably with the FAVOR and API-579 methods.

Critique of Technical Basis Work

Two calculations were scrutinized: (1) applying the RG 1.161 procedure to calculate a required USE for a range of vessel geometries and (2) applying the FAVOR code to calculate a required USE for a range of vessel geometries. The QA task involved interviews with the staff member who performed the technical basis (TB) work as well as confirmatory calculations.

RG 1.161 Method

The interviews revealed one issue of concern for the RG 1.161 calculations: the crack stability criterion (Equation 2) was not employed in the TB work. As a matter of technical rigor, the crack stability criterion should always be included in the calculations, since the safety factor for that criterion is higher than that for the non-initiation criterion (Equation 1). The results of these calculations from the TB work and QA work are compared in Figure 6 (a) and (b), respectively.

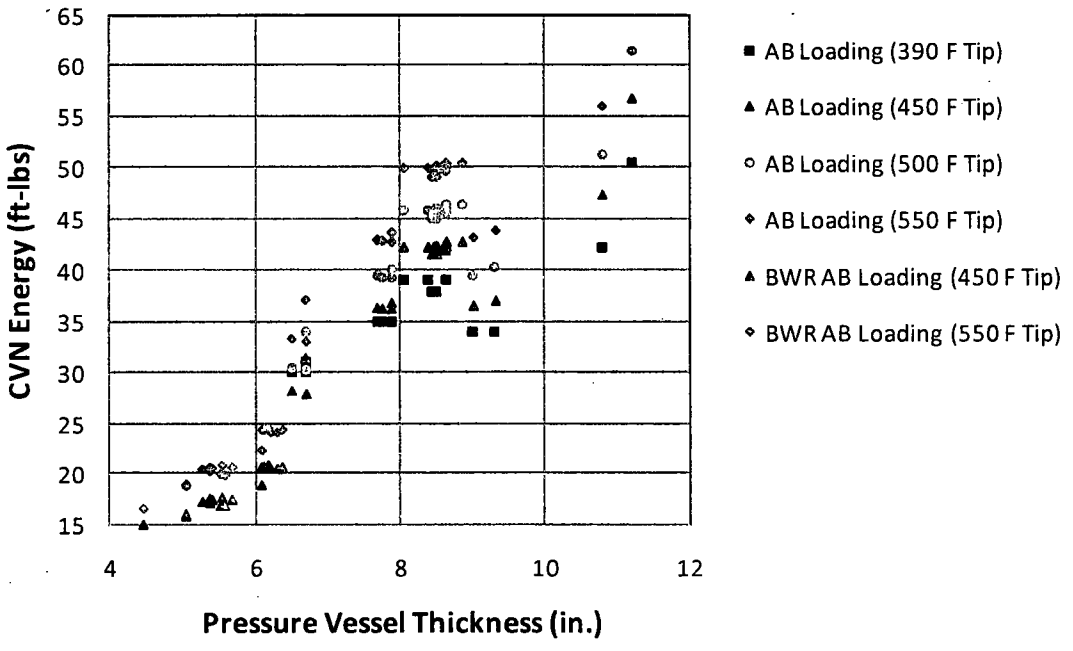

(a)

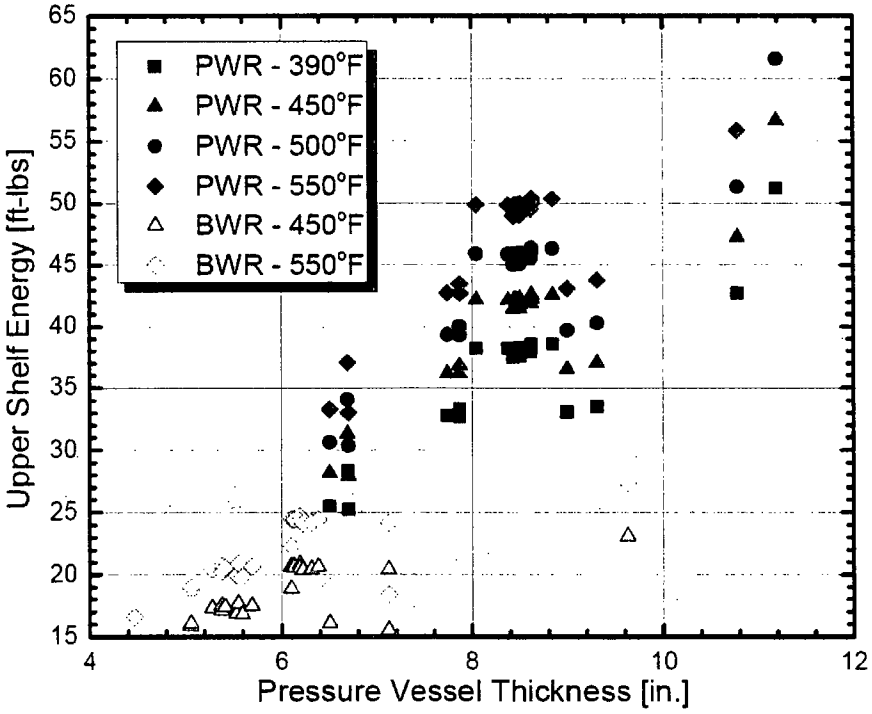

(b)

Figure 6: Required USE calculated according to RG 1.161 for (a) TB work and (b) QA work.

The results from the QA work (which accounted for crack stability) compare well with the results from the TB work, demonstrating the fact that the non-initiation criterion plays a dominant role in determining required USE. The issue raised by the QA work, therefore, has little effect on the results of this calculation.

FAVOR Method

Equation 9 is highly sensitive to temperature input, so the TB work proposed a method to justify T. Using the FAVOR code to determine required USE involves extracting crack tip temperature and applied SIF as functions of time from deterministic FAVOR runs that simulate a cooldown transient. The TB work then substituted the extracted SIF, which accounts for both internal pressure and thermal stress, into equation 8 to estimate the applied J. This procedure neglects the small scale yielding correction represented by Equation 7. The small scale yielding correction can increase the calculated J value by about 9% compared to J calculated without the correction, so the TB method of estimating J from FAVOR introduces a source of error in the calculation of USE. J_R is estimated from the FAVOR results by substituting crack tip temperature into Equation 10. This calculation procedure leads to J and J_R vs. time for a given CVN, as exemplified in Figure 2.

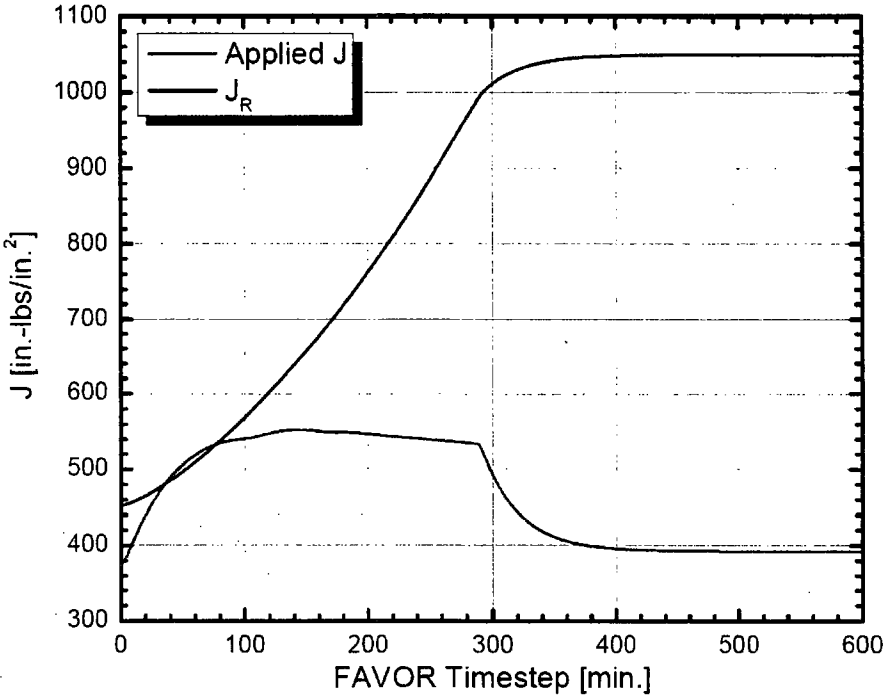

Figure 2: Example of J and J_R determined from FAVOR results.

The CVN value that leads to J and J_R tangent is then taken to be the required minimum USE. The USE was calculated by an iterative method where J_R was calculated with successively smaller values of CVN until the two curves were approximately tangent. The USEs determined via the FAVOR method were then compare to that determined by RG 1.161 procedures, in order to validate the correct crack tip temperature. The FAVOR results and RG 1.161 results at 450°F crack tip temperature are compared in Figure 3 (a) and (b) as determined during the TB work and QA work, respectively.

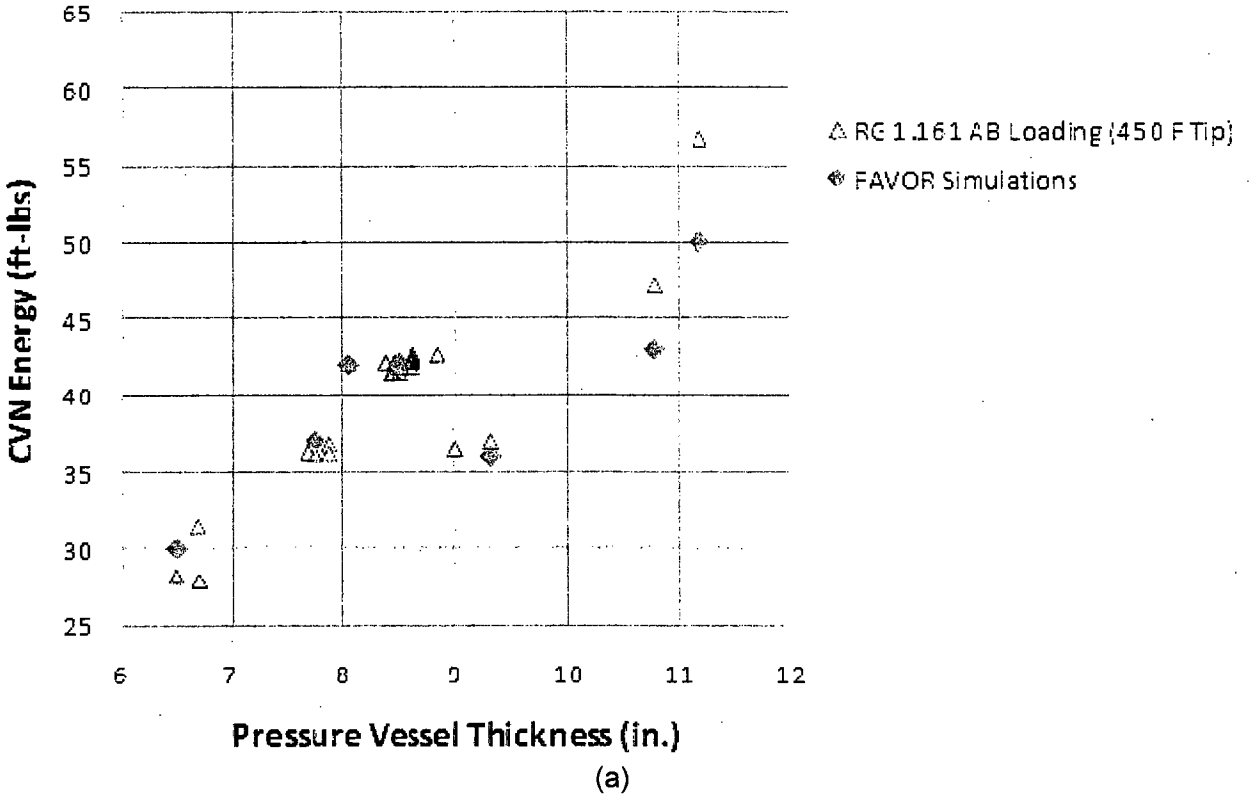

(a)

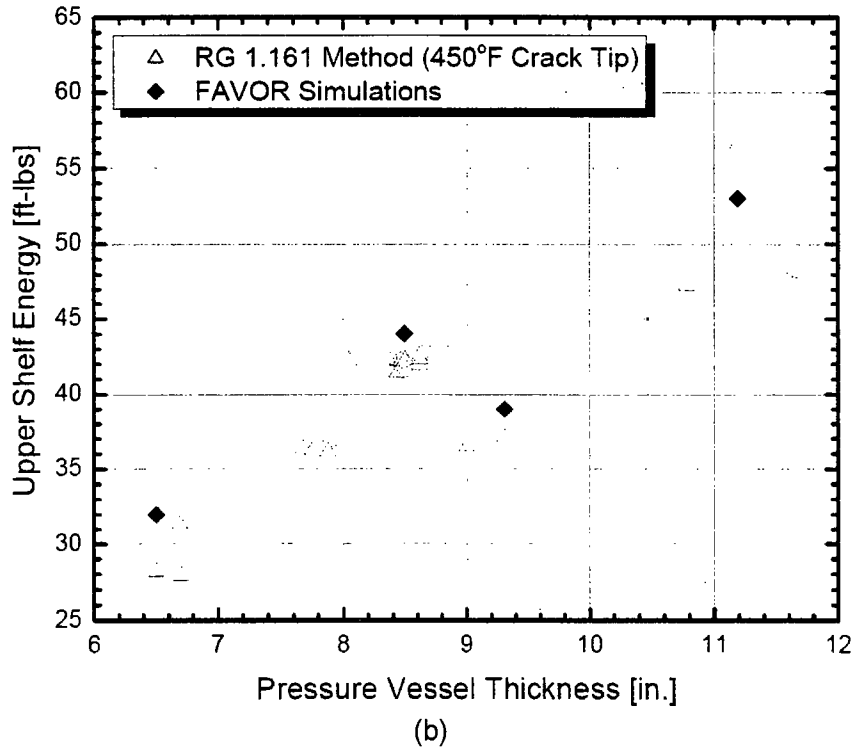

(b)

Figure 3: Comparison of required USE obtained from the RG 1.161 and FAVOR methods for (a) the TB work and (b) the QA work.

The QA calculations included a factor of 1.09 in the applied J calculation, in order to account for the small scale yielding correction. For the purposes of calculating required USE, this procedure is not recommended. For the purposes of the QA work, however, it provides a method to assess the error introduced by neglecting the small scale yielding correction. A comparison of Figures 3 (a) and (b) shows that the required USE is increased by roughly 3 ft-lbs when accounting for small scale yielding. The main conclusion of the TB regarding this work (i.e., that 450°F is the correct temperature input to J_R model) remains valid, since the results of the FAVOR simulations match closely with the results of the RG 1.161 calculation.

In the TB work, the RG 1.161 USE results obtained with T = 450°F were plotted against the proposed thickness-dependent USE limit, which is described by Equation 18.

$$Minimum\ USE = \begin{cases} 35\ ft-lbs & if\ \ t \le 7\ in. \\ 35 + 5(t-7)\ ft-lbs & if\ 7\ in. < t < 10\ in. \\ 50\ ft-lbs & if\ t \ge 10\ in. \end{cases} \qquad \text{Equation 18}$$

The proposed minimum USE, along with the confirmatory results from RG 1.161, are shown in Figure 4 (a) and (b) for the TB work and QA work, respectively.

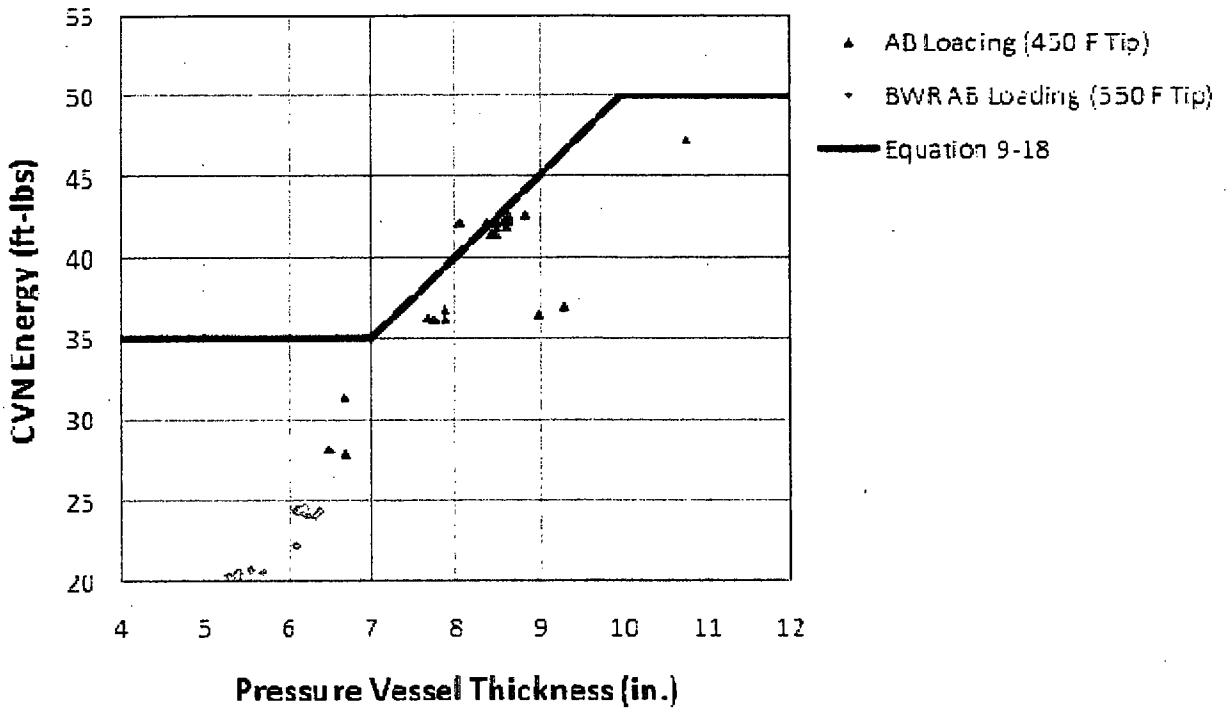

(a)

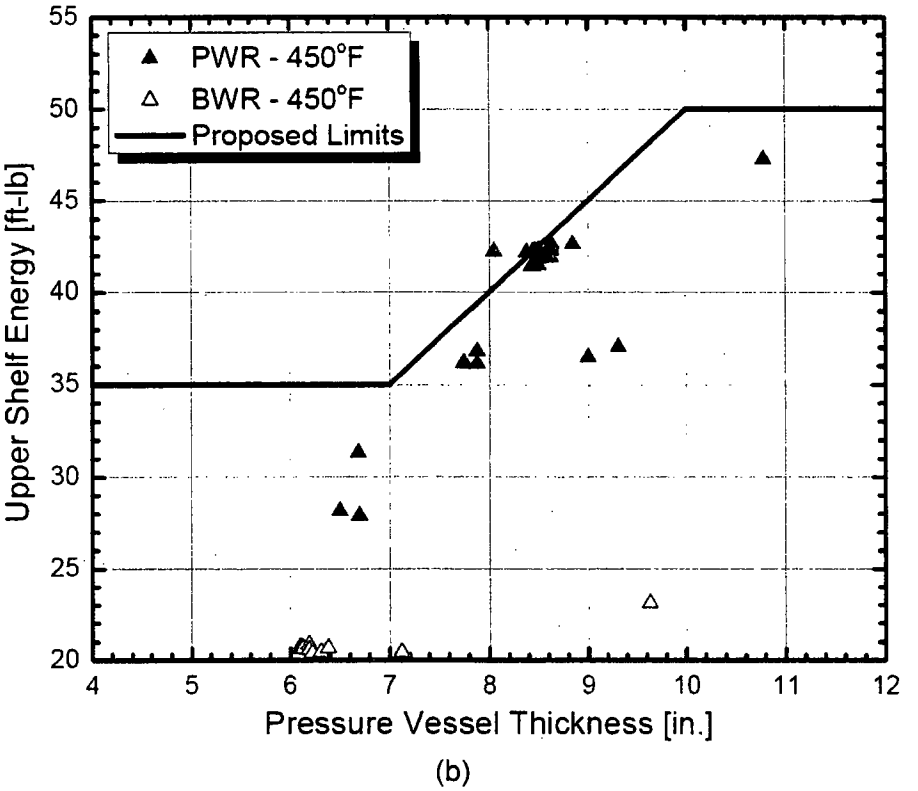

(b)

Figure 4: Proposed USE limits plotted with results from RG 1.161 calculations: (a) TB work, (b) QA work.

Figures 4(a) and (b) show reasonable agreement.

Comment on Figure

The draft TB for the minimum USE shows Figure 5 to demonstrate a situation where the crack stability criterion is not met.

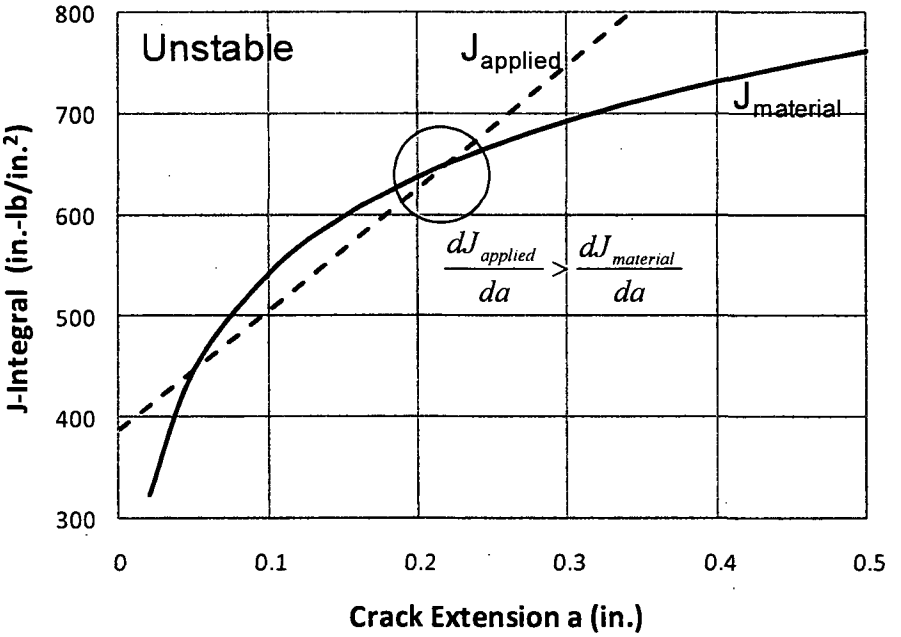

Figure 5: Figure reference in draft TB to demonstrate a situation where the crack stability criterion is violated.

In fact, Figure 5 illustrates a situation that meets the crack stability criterion, since there is a portion of the driving force curve (i.e, applied J) that lies below the resistance curve (i.e., $J_{material}$ in the figure, or J_R). While the slope of J is indeed greater than the slope of J_R at the point circled, the correct intersection point to perform this evaluation is the one located at lower crack extension. This concept can be confirmed by considering a figure from a fracture mechanics text (Figure 6).

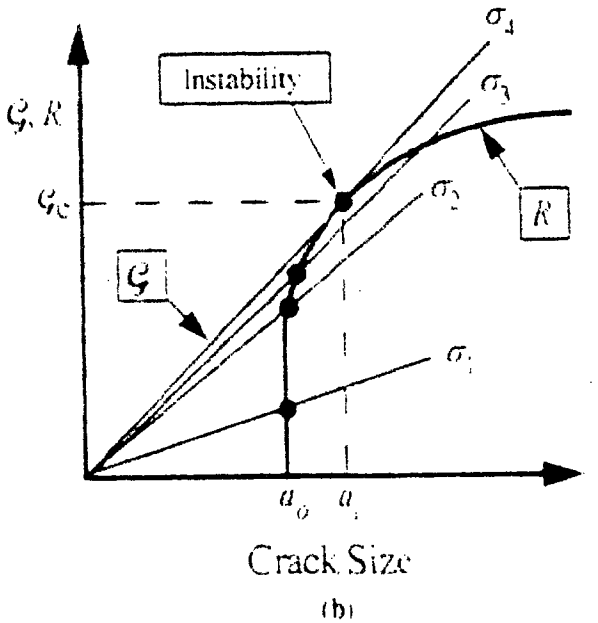

Figure 6: Demonstration of crack stability.

Figure 6 shows that instability begins when the driving force curve is tangent to the resistance curve. When the driving force curve is secant to the resistance curve, the crack is stable.

Conclusions

The results of the QA effort for USE support the following conclusions.

1. The K_p and K_{th} equations (Equations 1 and 5, respectively), while originally developed for only PWR vessel geometry, were verified for use for BWR vessel geometry.
2. While the TB work incorrectly neglected the crack stability criterion for the RG 1.161 calculations, modifying the analysis to account for crack stability does not change the results of the analysis.
3. The proposed procedure to calculate J from FAVOR results neglects the small-scale yielding correction (Equation 7), which can increase the calculated J by 9%.
4. After adjusting the calculated J results by a factor of 1.09 to account for small scale yielding, the results still confirm the original conclusion from the draft TB: 450°F is an appropriate crack tip temperature to use for the RG 1.161 calculations.
5. Figure 5 should not be included in the TB to demonstrate instability, since it actually demonstrates stability.
6. The proposed thickness-dependent USE limit was independently verified by the QA work.